Magnetostructural study of substituted α-nitronyl aminoxyl radicals with chlorine and hydroxy groups as crystalline design elements

Oriol Jürgens, Joan Cirujeda, Montse Mas, Ignasi Mata, Araceli Cabrero, José Vidal-Gancedo, Concepció Rovira, Elies Molins and Jaume Veciana*

Institut de Ciència de Materials de Barcelona (CSIC), Campus de la UAB, 08193-Bellaterra, Barcelona, Spain

We present a new family of phenyl substituted α-nitronyl aminoxyl radicals which contain hydroxy- and chlorine-substituents as crystal engineering tools. The magnetic behaviour of these radicals strongly differs in dimensionality and strength, showing in all cases antiferromagnetic interactions. We have determined the X-ray crystal structure and analysed the crystal packings of these radicals. From this analysis all the observed magnetic properties can be conveniently rationalized by only considering the close contacts of NO groups of neighbouring molecules according to the generally accepted mechanisms for intermolecular magnetic interactions. Beside the strong O—H···O(—N) hydrogen bonds and the weaker C—H···O(—N) hydrogen bonds, weak Cl···H bonds also seem to play a significant role in determining the molecular arrangement in the solid state and, therefore, the magnetic properties. In only one case are close Cl···Cl contacts observed, pointing to attractive interactions between chlorine atoms.

Magnetic properties of molecular solids depend both on the molecular electronic properties and on the intermolecular electronic interactions present in the solid state. Since the discovery of the *β*-phase of 4-nitrophenyl α-nitronyl aminoxyl,† the first example of a purely organic free radical with a bulk ferromagnetic transition,[1] much work has been devoted to the design of new substituted α-nitronyl aminoxyl radicals as building blocks for new molecular magnetic materials and bonding through OH substituents has been demonstrated to be a powerful crystal engineering element of α-nitronyl aminoxyl radicals providing new supramolecular architectures with relevant magnetic properties.[2] One of these new molecular solids was obtained with 4-hydroxyphenyl α-nitronyl aminoxyl radical.[3] This radical in the solid state forms a two-dimensional network built up by O—H···O(—N) and C—H···O(—N) hydrogen bonds that explains its quasi-two-dimensional ferromagnetic behaviour. On the other hand the 2-hydroxyphenyl and 2,5-dihydroxyphenyl α-nitronyl aminoxyl radicals[4,5] undergo bulk ferromagnetic transitions at 0.45 and 0.5 K, respectively, being two of the rare examples of purely organic ferromagnets. Beside their crystal packing, which is controlled by a complex network of weak C—H···O(—N) hydrogen bonds, the twist angles between the phenyl rings and the mean planes defined by the ONCNO groups seem to play a significant role in determining this unusual magnetic property. Therefore such results clearly show that the control of the molecular conformation and the crystal packing are key points in molecular magnetism.

Chlorine atoms have long been known for their steering ability in crystal engineering of molecular solids. Attractive Cl···Cl interactions and C—H···Cl hydrogen bonds have been described as responsible for this ability.[6,7] Herein we report a detailed magnetostructural study of a new family of phenyl α-nitronyl aminoxyl radicals **3–5** that combine OH groups and Cl atoms, attached to different positions of the phenyl rings, as crystalline design elements. The combination of these two crystalline design elements has provided an effective way to modulate the crystal packing of several chlorine substituted phenols,[8,9] leading to interesting applications to magnetic molecular solids.

† α-Nitronyl aminoxyl is used throughout to indicate 4,5-dihydro-4,4,5,5-tetramethyl-3-oxido-1*H*-imidazol-3-ium-1-oxyl.

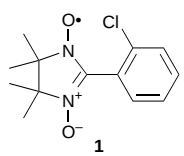

1

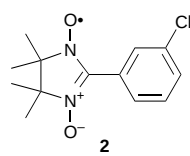

2

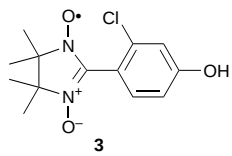

3

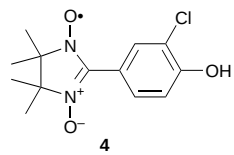

4

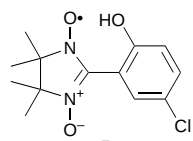

5

Radicals with only one Cl atom at the *ortho* and *meta* positions, radicals **1** and **2**, have also been studied here as reference compounds in order to evaluate the role played by this bulky and electroactive atom in crystal packing. Interestingly, the radical with one Cl atom at the *ortho* position also provides an opportunity to evaluate the effect of a large torsion between the two rings of the radical without introducing any strong O—H···O(—N) hydrogen bonds.

Experimental

General procedures

Radicals **1–5** were prepared using the procedure described by Ullman and co-workers.[10] The 2,3-(dihydroxylamino)-2,3-dimethylbutane used as a precursor was obtained by following the reported procedure.[11] Melting points were determined by differential scanning calorimetry (Perkin-Elmer, DSC-7 calorimeter) and are given as the maxima of the observed peaks. All radicals containing OH groups, radicals **3–5**, melt with decomposition. IR (Nicolet 710 FT-IR spectrometer) and UV–VIS spectra (Cary 5 UV–VIS-NIR spectrometer) of the synthesized radicals were also recorded.

Synthesis of free radicals

2-(2-Chlorophenyl)-4,5-dihydro-4,4,5,5-tetramethyl-3-oxido-1*H*-imidazol-3-ium-1-oxyl 1. 2,3-(Dihydroxylamino)-2,3-dimethylbutane (2.11 g; 14.2 mmol) was added to a stirred solution of 2-chlorobenzaldehyde (2 g; 14.2 mmol) in 30 ml of methanol. Stirring at room temp. was continued for 20 h and the resulting white precipitate was filtered off and dried *in vacuo*. This solid was oxidized with a solution of $NaIO_4$ (1.5 g; 7.1 mmol) in 50 ml of water at 5 °C and extracted with dichloromethane. The solution was evaporated and the crude product was purified by column chromatography (SiO_2) with ethyl acetate dichloromethane (1:1) as eluent (2.55 g; yield, 67% from the aldehyde). Single crystals of **1** were grown by evaporation at room temp. from a toluene solution. Mp 168.3 °C (Found: C, 58.27; H, 6.02; N, 10.42. Calc. for $C_{13}H_{16}N_2O_2Cl$: C, 58.32; H, 6.02; N, 10.46%); ν_{max}/cm^{-1} (KBr) 1595w, 1449m, 1404s, 1367s, 1211w, 1171m, 1133m, 1055m, 766m; UV–VIS (CH_2Cl_2) λ_{max}/nm (ε): 354 (18 000), 554 (780); MS (EI) *m/z*: 267 (M^+), 179, 138, 114, 84, 69, 56.

2-(3-Chlorophenyl)-4,5-dihydro-4,4,5,5-tetramethyl-3-oxido-1*H*-imidazol-3-ium-1-oxyl 2. Radical **2** was synthesized by the same procedure as **1**. Crystals were grown by slow evaporation of a heptane–dichloromethane (10:1) solution at room temp. Mp 123.5 °C (Found: C, 58.30; H, 6.01; N, 10.40. Calc. for $C_{13}H_{16}N_2O_2Cl$: C, 58.32; H, 6.02; N, 10.46%); yield, 92% from the aldehyde; ν_{max}/cm^{-1} (KBr) 1580m, 1418m, 1395m, 1364s, 1134m, 795m; UV–VIS (CH_2Cl_2) λ_{max}/nm (ε): 271 (16 000), 367 (18 000), 584 (480); MS (EI) *m/z*: 267 (M^+), 179, 138, 114, 84, 69.

2-(2-Chloro-4-hydroxyphenyl)-4,5-dihydro-4,4,5,5-tetramethyl-3-oxido-1*H*-imidazol-3-ium-1-oxyl 3. Radical **3** was obtained in a similar way to **1**, but instead of stirring the reactants, they were refluxed in benzene for 19 h. All attempts to grow large single crystals of radical **3** failed, and so its X-ray structure could not be determined. Mp 166.2 °C (decomp.) (Found: C, 55.21; H, 5.75; N, 9.70. Calc. for $C_{13}H_{16}N_2O_3Cl$: C, 55.03; H, 5.68; N, 9.87%); yield, 22% from the aldehyde; ν_{max}/cm^{-1} (KBr): 1604s, 1456m, 1364m, 1106m, 858w; UV–VIS (CH_2Cl_2) λ_{max}/nm (ε): 269 (13 000), 328 (12 000), 561 (1040); MS (EI) *m/z*: 283 (M^+), 195, 153, 114, 84, 69.

2-(3-Chloro-4-hydroxyphenyl)-4,5-dihydro-4,4,5,5-tetramethyl-3-oxido-1*H*-imidazol-3-ium-1-oxyl 4. Radical **4** was synthesized by the same procedure as for **3**. Crystals were grown by a slow diffusion of pentane into a concentrated toluene solution at room temp. Mp 158.4 °C (decomp.) (Found: C, 55.31; H, 5.75; N, 9.81. Calc. for $C_{13}H_{16}N_2O_3Cl$: C, 55.03; H, 5.68; N 9.87%); yield, 93% from the aldehyde; ν_{max}/cm^{-1} (KBr): 1605m, 1490m, 1387m, 1340s, 1300m, 1273m, 1214m, 1169m, 1133m, 831m, 702w, 541w; UV–VIS (CH_2Cl_2) λ_{max}/nm (ε): 282 (16 000), 369 (12 000), 618 (720); MS (EI) *m/z*: 283 (M^+), 195, 153, 114, 84, 69.

2-(5-Chloro-2-hydroxyphenyl)-4,5-dihydro-4,4,5,5-tetramethyl-3-oxido-1*H*-imidazol-3-ium-1-oxyl 5. Radical **5** was obtained similarly to **3**. Crystals were grown by slow evaporation of a heptane–dichloromethane (10:1) solution at room temp. Mp 118.7 °C (decomp.) (Found: C, 55.78; H, 5.94; N, 9.05. Calc. for $C_{13}H_{16}N_2O_3Cl$: C, 55.03; H, 5.68; N, 9.87%); yield, 25% from the aldehyde; ν_{max}/cm^{-1} (KBr): 1573w, 1471s, 1375m, 1341m, 1278m, 1135m, 825m, 646w; UV–VIS (CH_2Cl_2) λ_{max}/nm (ε): 349 (4400), 581 (440); MS (EI) *m/z*: 283 (M^+), 195, 153, 114, 84, 69.

Magnetic measurements

DC magnetic susceptibility data from 2 to 300 K, in a magnetic field of 1 T, were collected using a 'Quantum Design' MPMS Superconducting SQUID susceptometer and using microcrystalline samples (80–115 mg) of the radicals **1–5**. The diamagnetic contributions of the sample holder and the radicals were determined by extrapolation from the χT *vs.* T plots in the high-temperature range and were used later to correct the SQUID outputs.

X-Ray measurements

X-Ray data for single crystals of **1, 2, 4** and **5** were collected at 293 K on an Enraf-Nonius CAD 4 FR-590 diffractometer working at 1 kW with monochromatic Mo-Kα ($\lambda = 0.71069$ Å) radiation. Data were collected by using an $\omega/2\theta$ scan method. The structures were all refined by a full-matrix least squares method which minimized $\Sigma w(\Delta F)^2$.‡ The presence of different polymorphs in each crystalline material used for magnetic measurements was ruled out by means of powder X-ray diffraction spectra by comparing the experimental spectra with the simulated ones based on the single crystal X-ray diffraction structure. These spectra were simulated by using the CERIUS2 2.0 program (Molecular Simulations Inc.). Powder diffraction spectra were collected on a Rigaku Dimax RC-200 diffractometer with a 12 kW rotating anode generator and a monochromator of single crystalline graphite for Cu-Kα radiation.

EPR spectroscopic measurements

The EPR spectra of radicals **1–5** in toluene solutions under free tumbling conditions were recorded on a Bruker ESP-300E spectrometer operating in the X-band (9.3 GHz) with a rectangular TE102 cavity and equipped with a field-frequency (F/F) lock accessory and a built-in NMR gaussmeter. Signal-to-noise ratio was increased by accumulation of scans using the F/F lock accessory to guarantee a high-field reproducibility. Precautions to avoid undesirable spectral line broadening such as that arising from microwave power saturation and magnetic field overmodulation were taken. In order to avoid dipolar broadening, the radical solutions were carefully degassed by bubbling with pure argon.

Results and Discussion

Spin density distribution of the radicals

The most widely accepted mechanism for rationalizing the intermolecular magnetic interactions in organic molecular solids is the so-called McConnell I mechanism based on the overlap of the orbitals on atoms with large spin densities of neighbouring molecules.[12,13] According to this mechanism, dominant contacts of atoms with spin densities having the same sign produce an antiferromagnetic interaction between the two neighbouring molecular units. In contrast, ferromagnetic interactions are favoured if opposite signs in these contacts are predominant. For this reason it is important in magnetic molecular materials to know how the spin density of the unpaired electron is distributed within the building block molecules.

Free tumbling solution EPR spectra provide the necessary information about such spin density distributions in organic free radicals, through the determination of the coupling constants with the magnetically active nuclei of the molecules. The EPR spectra of radicals **1–5** show basically five main groups of lines with relative intensities of 1:2:3:2:1, resulting from the coupling of the unpaired electron with two equivalent nitrogen nuclei ($I = 1$), as shown in Fig. 1(*a*) for radical **4**. The

‡ Atomic coordinates, thermal parameters, and bond lengths and angles have been deposited at the Cambridge Crystallographic Data Centre (CCDC). See Information for Authors, *J. Mater. Chem.*, 1997, Issue 1. Any request to the CCDC for this material should quote the full literature citation and the reference number 1145/40.

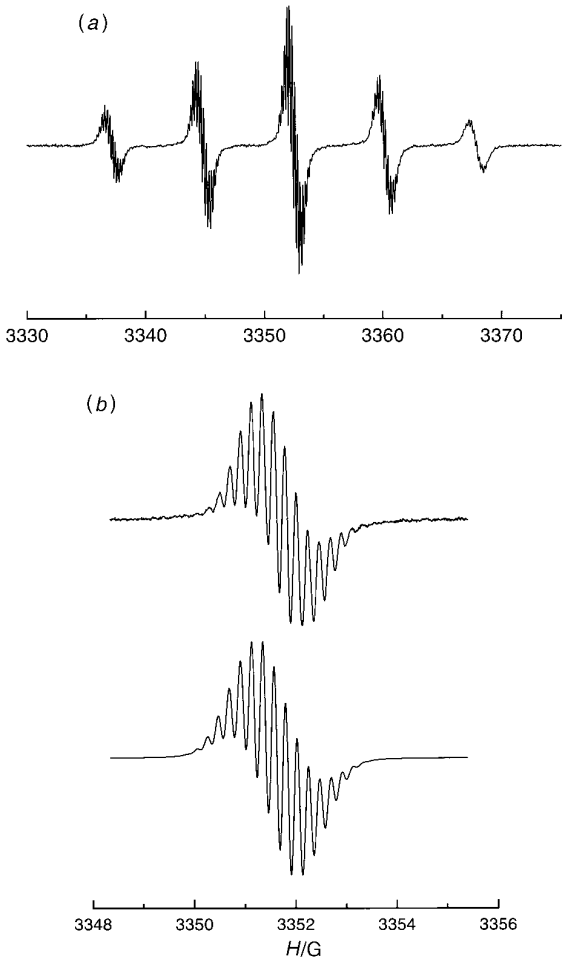

Fig. 1 (*a*) Complete EPR spectrum of radical **4** in toluene at 293 K. (*b*) Experimental (upper) and simulated (lower) central groups of EPR lines. The computer simulation was carried out using a Lorentzian line shape with $\Delta H_{1/2}$ of 0.13 G and the hfcc valves given in Table 1.

values of the isotropic hyperfine coupling constants in all cases are between 7.2 and 7.8 G; *i.e.* $a_N = 7.5(3)$ G; which is typical for freely tumbling substituted α-nitronyl aminoxyl radicals.[1,14,15] A more detailed analysis of these five main groups of signals reveals a complex pattern of lines arising from supplementary couplings with the twelve equivalent hydrogen atoms ($I = 1/2$) of the four methyl groups and all the hydrogen atoms of the phenyl ring.

Computer simulations of the experimental EPR spectra of **1–5** yield the hyperfine coupling constants summarized in Table 1. All values are in agreement with those previously reported for other α-phenyl nitronyl aminoxyl radicals,[15] indicating, therefore, that the chloro- and hydroxy-substituents do not alter the electron distribution in the radicals significantly. Consequently, the unpaired electron is mainly distributed on both NO groups and the α-carbon atom. This result is in agreement with those previously reported by other authors,[16] who have determined by NMR measurements that the N and O atoms carry a large and positive spin density while the α-carbon atom has a significant negative spin density. The methyl groups and the aromatic ring also carry a spin density, as inferred from the observed EPR hyperfine couplings with all these hydrogen atoms. The coupling constants for the aromatic hydrogen atoms are smaller in radicals **1**, **3** and **5** than in radicals **2** and **4**. The loss of planarity between the five- and the six-membered rings, due to the presence of a substituent at the *ortho* position in compounds **1**, **3** and **5**, yields a satisfactory explanation for this fact. Assignments of the coupling constants of aromatic hydrogen atoms for radicals **1–5** have been performed by comparison with a whole series of radicals with non-magnetically active substituents located at different positions of the phenyl rings.[17]

Molecular and crystal structures of radicals

General crystallographic information for radicals **1**, **2**, **4** and **5** is summarized in Table 2. Atomic numbering schemes used for these radicals are shown in Fig. 2 together with their molecular conformations.

Structure of radical 1. Radical **1** crystallizes in the orthorhombic system with an asymmetric unit which contains one radical molecule. The most relevant feature of the solid state molecular conformation of radical **1** is the large angle (62°) formed by the phenyl ring and the mean plane of the O—N—C—N—O unit. This twist angle is larger than that reported for the unsubstituted phenyl α-nitronyl aminoxyl radical (29°)[18] as well as for the *p*-chloro- (24°),[19] the *o*-hydroxy- (40°)[4] and the *p*-hydroxyphenyl- (30°)[3a] substituted examples. Therefore, this result suggests that the large angle in **1** is merely due to steric hindrance of the bulky Cl atom at the *ortho* position.

The intramolecular Cl···O distance in radical **1** (3.24 Å) is quite similar to intermolecular distances found between halogen and nucleophile atoms by Murray-Rust and co-workers.[20] This fact suggests that, in spite of the strong steric hindrance between the Cl and the O atom, a slightly attractive interaction between both atoms cannot be excluded. The measured distance would be the resulting equilibrium position between the steric repulsion and such halogen–nucleophile attracting forces. In our case, the C—Cl···O angle is obviously much smaller

Table 2 Crystallographic data for radicals **1**, **2**, **4** and **5**

compound	**1**	**2**	**4**	**5**
a/Å	10.483(3)	9.946(2)	13.735(1)	9.741(6)
b/Å	10.921(3)	11.522(1)	11.819(2)	11.663(5)
c/Å	11.671(3)	12.700(2)	17.153(3)	13.324(14)
β/°	—	109.91(1)	—	111.23(7)
data/parameters	3887/165	4130/213	2441/176	2037/223
V/Å^3	1336.2(6)	1368.4(4)	2785.5(7)	1411(2)
D_c/g cm^{-3}	1.331	1.300	1.354	1.336
space group	$P2_12_12_1$	$P2_1/c$	*Pbca*	$P2_1/n$
Z	4	4	8	4
R	0.0394	0.0478	0.0514	0.0488

Table 1 Summary of hyperfine coupling constants (*a*/G; 1 G = 10^{-4} T) obtained for radicals **1–5** by computer simulation of the EPR spectra of toluene solutions

compound	a_N	a_H(methyl)	a_H(*ortho*)	a_H(*meta*)	a_H(*para*)
1	7.26 (2N)	0.20 (12H)	0.24	0.15, 0.12	[a]
2	7.40 (2N)	0.19 (12H)	0.52 (2H)	0.21	0.43
3	7.65 (2N)	0.18 (12H)	0.23	0.16 (2H)	—
4	7.50 (2N)	0.21 (12H)	0.54, 0.50	0.17	—
5	7.81, 7.40	0.20 (12H)	0.33	0.25	0.30

[a]Not observed.

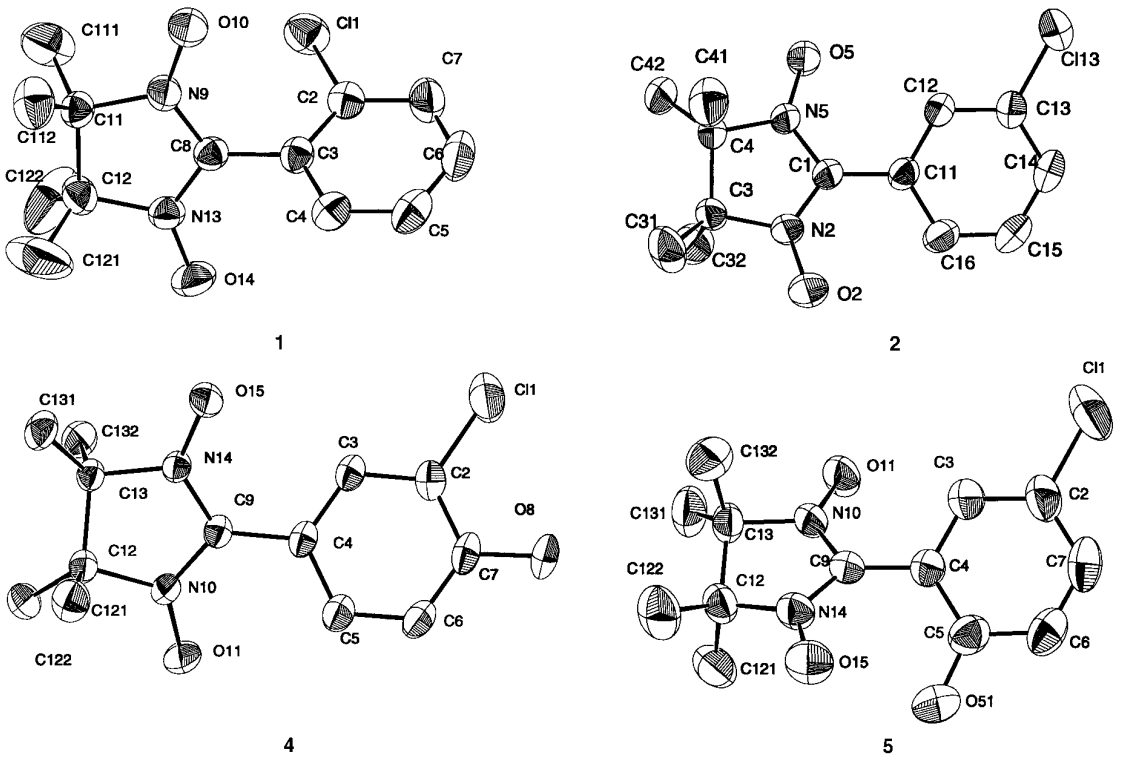

Fig. 2 Molecular conformations of radicals **1**, **2**, **4** and **5** with the atomic numbering schemes used in the text and tables

(75°) than in the examples described by Murray-Rust and coworkers[20] because of the intramolecular nature of that contact.

As shown in Fig. 3, the molecules of radical **1** are packed in such a way that one of the two NO groups of each molecule forms a hydrogen bond with a methyl group of a neighbouring molecule [d(H11D···O14^{i}, i = $-x$, $1/2+y$, $5/2-z$) = 2.64 Å; θ(C112—H11D···O14^{i}) = 154°] giving rise to twisted chains along the b axis. Each of these chains is connected to two neighbouring chains by means of C_{arom}—H7···O14^{ii}—N13^{ii} hydrogen bonds [ii = $1/2+x$, $1/2-y$, $2-z$; d(H7···O14^{ii}) = 2.66 Å; θ(C7—H7···O14^{ii}) = 130°] forming molecular sheets

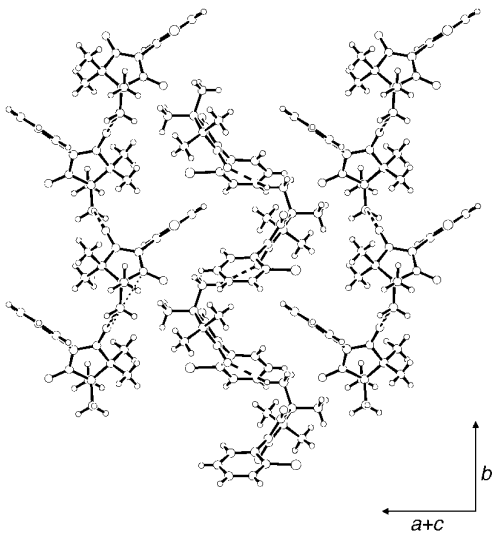

Fig. 3 Crystal packing of radical **1**. Crystallographic (1 0 −1) plane formed by chains of molecules connected through C_{methyl}–H11D···O14^{i}–N13^{i} (i = $-x$, $1/2+y$, $5/2-z$) hydrogen bonds (dashed lines) along the b axis. The dotted line connects the nearest NO groups of different molecules, N13–O14···N9^{iv} (iv = $-x$, $-1/2+y$, $-5/2-z$).

perpendicular to the crystallographic [1 0 −1] direction. Between adjacent planes no H···O contacts with d(H···O) < 3 Å are observed. Molecules of adjacent planes are just connected by weak C_{methyl}—H11B···C11^{iii} interactions [iii = $-x$, $1/2+y$, $3/2-z$; d(H11B···C11^{iii}) = 3.01 Å; θ(C111—H11B···C11^{iii}) = 172°], and these interactions are propagated along the b axis.

As a result of this complex crystal packing, the shortest distance between the NO groups of different molecules [d(O14···N9^{iv}) = 4.94 Å; iv = $-x$, $-1/2+y$, $-5/2-z$; d(O14···O10^{iv}) = 5.39 Å] occurs between neighbouring molecules in the chains along the b axis. These kinds of contacts are responsible for the magnetic behaviour as will be discussed below.

Structure of radical 2. This compound crystallizes in the monoclinic $P2_1/c$ space group with an asymmetric unit containing one radical molecule. Fig. 2 shows its solid state molecular conformation. The torsion angle between the two rings of radical **2** is 26°, being very similar to those of other radicals with similar steric requirements at the *ortho* position.[18,19,3a] The crystal structure of **2** clearly shows alternating planes perpendicular to the crystallographic [1 0 −1] direction. Within these planes, the molecules are connected to each other forming chains along the b axis [see Fig. 4(*a*)] by means of C_{arom}—H14···O2^{i}—N2^{i} hydrogen bonds [i = $1-x$, $-1/2+y$, $1/2-z$; d(H14···O2^{i}) = 2.47 Å; θ(C14—H14···O2^{i}) = 129°]. These chains are linked to each other by weak C_{methyl}—H44···O5^{ii}—N5^{ii} hydrogen bonds [ii = $-x$, $1/2+y$, $-1/2-z$; d(H44···O5^{ii}) = 2.55 Å; θ(C42—H44···O5^{ii}) = 148°].

As happens with radical **1**, between adjacent planes containing the stronger C—H···O hydrogen bonds, no other H···O contacts with d(H···O) < 3 Å are observed. In a similar way as occurs with radical **1** there are C_{arom}—H15···C113^{iii} interactions [iii = x, $1/2-y$, $1/2-z$; d(H15···C113^{iii}) = 3.12 Å; θ(C15—H15···C113^{iii}) = 154°] between the planes. Also, between chains of neighbouring (1 0 −1) planes, we have found short C113···C113^{iv} contacts [iv = $1-x$, $-y$, $-z$;

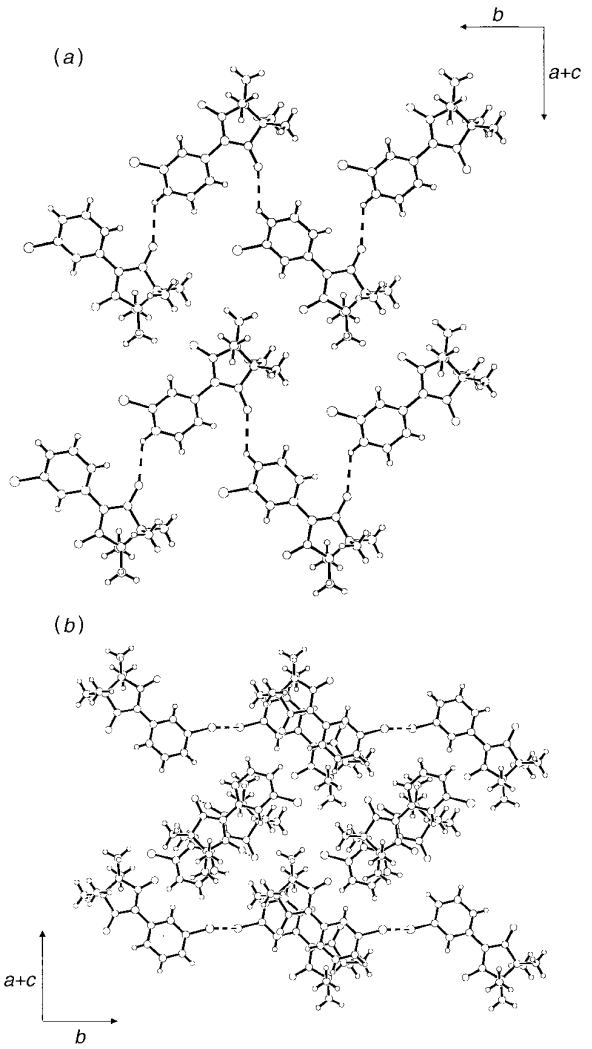

Fig. 4 Crystal packing of radical **2**. (*a*) Crystallographic (1 0 −1) plane formed by chains of molecules connected through C_{arom}–H14···O2^{i}–N2^{i} (i = 1 − *x*, −1/2 + *y*, 1/2 − *z*) hydrogen bonds (dashed lines) along *b* axis. (*b*) Molecules of two neighbouring (1 0 −1) planes showing as dashed lines C113···C113^{iv} close contacts (iv = 1 − *x*, −*y*, −*z*). The dotted lines connect the nearest NO groups of different molecules, N2···O5^{v}–N5^{v} (v = −*x*, 1 − *y*, −*z*).

d(C113···C113^{iv}) = 3.72 Å], which are depicted in Fig. 4(*b*). The distances of such contacts are in accordance with those described by Desiraju[7] for several other compounds which clearly show non-covalent attractive Cl···Cl interactions. Therefore this result suggests that the Cl···Cl interactions are driving forces for the packing of molecules in (1 0 −1) planes.

As will be discussed below, from the magnetic point of view, the most important aspect of the crystal packing of radical **2** is the presence of short intermolecular distances between the NO groups of two molecules in neighbouring (1 0 −1) planes. This kind of contact permits us to consider the molecular system as being composed of dimeric magnetic entities which are clearly shown in Fig. 4(*b*).

Structure of radical 4. Radical **4** crystallizes in the orthorhombic *Pbca* group and also contains one molecule in the asymmetric unit. In this case the phenyl ring is twisted with respect to the mean O—N—C—N—O plane by 28.5°. This result is again in accordance with the twist angles observed for other radicals with similar steric requirements, that is, those without substituents at the *ortho* positions.

The main feature of the crystal packing of radical **4** is the strong intermolecular O8—H8···O15^{i}—N14^{i} bond [i = 1 − *x*, −1/2 + *y*, 1/2 − *z*; *d*(H8···O15^{i}) = 1.72 Å; *θ*(O8—H8···O15^{i}) = 168°] which connects each molecule to two neighbours giving rise to zigzag chains along the *b* axis. This arrangement is reinforced by a second hydrogen bond [*d*(H6···O15^{i}) = 2.65 Å; *θ*(C6—H6···O15^{i}) = 128°] between the same NO group and an aromatic H atom in the *meta* position which is adjacent to the OH group which forms the strong hydrogen bond. Further, these chains are arranged into planes perpendicular to the crystallographic [1 0 0] direction by means of weak C_{methyl}—H134···O11^{ii}—N10^{ii} hydrogen bonds [ii = 1 − *x*, −*y*, −*z*; *d*(H134···O11^{ii}) = 2.71 Å; *θ*(C132—H134···O11^{ii}) = 160°], as shown in Fig. 5(*a*).

This pattern resembles very much the crystal packing reported for the 4-hydroxyphenyl α-nitronyl aminoxyl radical[3] but there are two basic differences caused by the presence of the Cl atom at the *meta* position. The first is that the rings of radical **4** are not coplanar to the (1 0 0) plane; *i.e.* the molecules are alternately canted within the chains. The second difference refers to the stacking of the planes along the crystallographic *a* direction, which in radical **4** takes place through C_{methyl}—H125···Cl1^{iii} interactions [iii = −1/2 + *x*, 1/2 − *y*, −*z*; d(H125···Cl1^{iii}) = 3.07 Å; *θ*(C122—H125···Cl1^{iii}) = 167°], C_{methyl}—H121···Cl1^{iv} interactions [iv = −1/2 + *x*, *y*, 1/2 − *z*; *d*(H121···Cl1^{iv}) = 3.08 Å; *θ*(C121—H121···Cl1^{iv}) = 134°] [shown in Fig. 5(*b*)] and C_{methyl}—H131···O11^{v}—N10^{v} hydrogen bonds [v = 1/2 − *x*, 1/2 + *y*, *z*; *d*(H131···O11^{v}) = 2.75 Å; *θ*(C131—H131···O11^{v}) = 151°], while in the *para*-hydroxy substituted radical the stacking of planes occurs through van der Waals interactions.

The lack of planarity of the molecules of radical **4**, within the twisted chains in the (1 0 0) plane, means that the shortest intermolecular distance between NO groups occurs pairwise

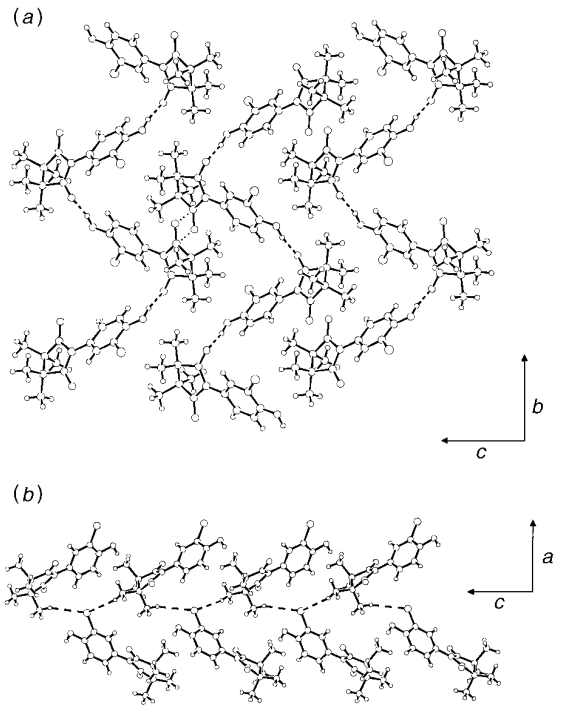

Fig. 5 Crystal packing of **4**. (*a*) Crystallographic (100) plane formed by zigzag chains of molecules connected through strong O8–H8···O15^{i}–N14^{i} (i = 1 − *x*, −1/2 + *y*, 1/2 − *z*) hydrogen bonds along *b* axis depicted as dashed lines. The dotted lines connect the nearest NO groups of different molecules, N10···O11^{vi}–N10^{vi} (vi = 1 − *x*, −*y*, −*z*). (*b*) Molecules of neighbouring (100) planes showing C_{methyl}–H125···C11^{iii} (iii = −1/2 + *x*, 1/2 − *y*, −*z*) and C_{methyl}–H121···C11^{iv} (iv = −1/2 + *x*, *y*, 1/2 − *z*) interactions which are depicted as dashed lines.

between molecules of neighbouring chains as shown in Fig. 5(*a*) leading to a dimeric magnetic pattern, as will be discussed below.

Structure of radical 5. This compound does not crystallize in the orthorhombic system, as occurs for radicals **1** and **4**, but in the monoclinic one, similarly to radical **2** which also has one chlorine atom in the *meta* position. The presence of the OH group at the *ortho* position results in the formation of a strong intramolecular O51—H51···O15—N14 hydrogen bond [d(H51···O15) = 1.66 Å; θ(O51—H51···O15) = 170°]. Consequently, there is a twist angle of 35° between the two rings of the molecule, as was also observed for the radical with one OH group in the *ortho* position.[4] Fig. 2 shows the molecular structure of **5**, where the lack of planarity is clear. Due to the establishment of these strong intramolecular O—H···O—N hydrogen bonds, the molecules are packed in the crystal through other types of weak hydrogen bonds. Thus, the molecules are arranged into zigzag chains parallel to the [1 0 1] direction by means of rather weak C_{arom}—H7···O11^{i}—N10^{i} hydrogen bonds [i = $-1/2+x$, $1/2-y$, $-1/2+z$; d(H7···O11^{i}) = 2.22 Å; θ(C7—H7···O11^{i}) = 157°]. The chains are layered into planes perpendicular to the [1 0 −1] direction by C_{methyl}—H13B···O15^{ii}—N14^{ii} hydrogen bonds [ii = $1/2+x$, $3/2-y$, $1/2+z$; d(H13B···O15^{ii}) = 2.82 Å; θ(C131—H13B···O15^{ii}) = 155°] as shown in Fig. 6(*a*).

Furthermore, the planes are connected pairwise through other C_{methyl}—H12A···O11^{iii}—N10^{iii} hydrogen bonds [iii = $1-x$, $1-y$, $1-z$; d(H12A···O11^{iii}) = 2.68 Å; θ(C121—H12A···O11^{iii}) = 174°] giving rise to an alternating pattern in which the radical molecules of two neighbouring planes form dimers, related by an inversion centre shown in Fig. 6(*b*). As will be seen below, these dimers are responsible for the magnetic behaviour of the compound.

As can be inferred from geometric considerations, all C—H···Cl distances present in this radical are longer than 3.3 Å. {The shortest ones are [d(H6···Cl1^{i}) = 3.33 Å; θ(C6—H6···Cl1^{i}) = 156°] and [d(H123···Cl1^{iv}) = 3.36 Å; θ(C122—H123···Cl1^{iv}) = 110.6°; iv = x, $1+y$, z]}.

The crystal packing of radical **5** is therefore very similar to the molecular arrangement of radical **2**. This result can be rationalized by noting that both compounds have similar crystalline design elements: in fact both radicals have one Cl atom at the *meta* position and the additional OH substituent at the *ortho* position of radical **5** seems to affect only the intramolecular conformation and not the intermolecular interactions. The fact that no Cl···Cl contacts are observed in radical **5** may be explained as a consequence of the lower planarity[7] of this molecule due to the OH substituent at the *ortho* position.

Summarizing the above structural analysis, the arrangement of molecules of the radicals **1**, **2**, **4** and **5** in the solid state is mainly governed by strong O—H···O—N (only possible in radicals **4** and **5**) and weak C—H···O—N hydrogen bonds giving rise to molecular solids with one- or two-dimensional structural character.[6,21] The C—H···Cl hydrogen bonds only seem to play an important role in the crystal packing of the radicals without OH substituents on the phenyl ring, as shown by the shorter H···Cl distances in radicals **1** and **2** compared with radicals **4** and **5**. Cl···Cl interactions have only been found for radical **2**. According to Desiraju *et al.*,[7] the lack of planarity, especially in radicals **1** and **5**, and the presence of other stronger intermolecular interactions, as occurs for **4**, may be responsible for the absence of Cl···Cl interactions in radicals **1**, **4** and **5**. As a consequence of such considerations, it has been observed that the placement of an additional Cl atom modulates considerably the crystal packing of phenyl α-nitronyl aminoxyl radicals.

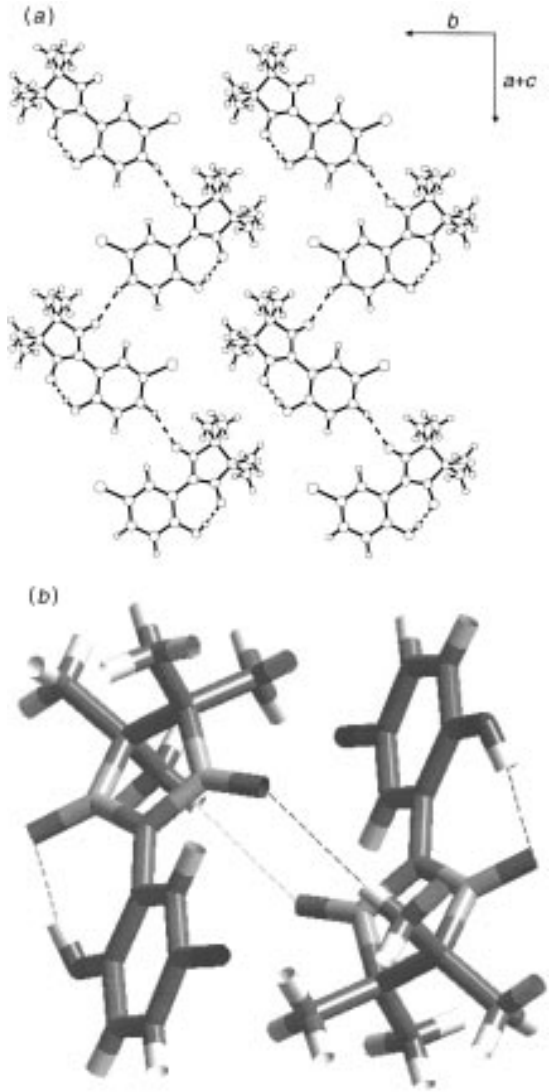

Fig. 6 Crystal packing of **5**. (*a*) Crystallographic (1 0 −1) plane formed by chains of molecules connected through C_{arom}–H7···O11^{i}–N10^{i} (i = $-1/2+x$, $1/2-y$, $-1/2+z$) hydrogen bonds parallel to the $a+c$ direction. (*b*) Molecules of two neighbouring (1 0 −1) planes forming dimers by intermolecular C_{methyl}–H12A···O11^{iii}–N10^{iii} (iii = $1-x$, $1-y$, $1-z$) hydrogen bonds. The strong intramolecular O51–H51···O15–N14 hydrogen bonds are also depicted.

Magnetic properties of radicals

Static magnetic susceptibility measurements of radicals **1–5** are shown in Fig. 7. Such measurements indicate that the molecular solids studied present in all cases intermolecular antiferromagnetic (AFM) interactions with different strengths. As we will discuss later, the magnetic dimensionalities vary from one compound to another in close relationship with their crystal packings.

The magnetic susceptibility data of **1** were nicely fitted to a 1D Heisenberg model of $S = 1/2$ molecular units having weak AFM interactions with a magnetic exchange interaction of $J/k_B = -0.95$ K. In the crystal structure of radical **1**, all the intermolecular distances between atoms carrying the larger spin densities are quite large. As described previously, the shortest one [d(O14···N9^{iv}) = 4.94 Å; iv = $-x$, $-1/2+y$, $-5/2-z$] occurs among atoms having a positive sign of spin density and that belong to molecules forming the previously described chains along the crystallographic b direction. In

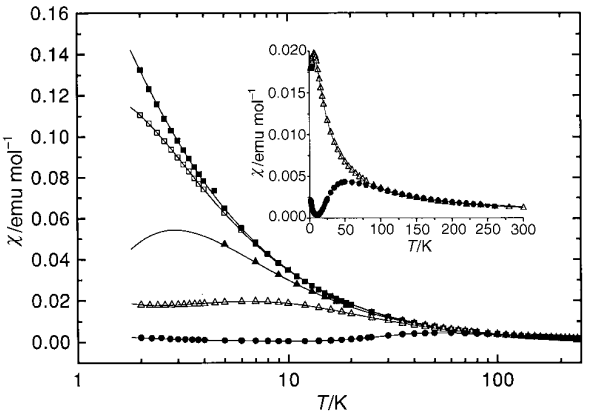

Fig. 7 Temperature dependence of the paramagnetic susceptibility χ of radicals (□) **1**, (▲) **2**, (■) **3**, (△) **4** and (●) **5**. The inset shows an enlargement of the temperature dependence for radicals **4** and **5**. The solid lines represent the fits of experimental data to the magnetic models explained in the text.

consequence, this molecular arrangement is in agreement with the observed weak 1D antiferromagnetic behaviour.

The magnetic behaviour of **2** is properly explained by a dimer model with antiferromagnetic interactions. However, the fitting of experimental data is considerably improved if an additional interdimer antiferromagnetic term is included in the Bleaney–Bowers equation for $S=1/2$ molecular units with an antiferromagnetic interaction of $J/k_B=-1.82$ K, by means of a temperature correction with a Weiss constant of $\theta=-1.39$ K.[22] This result means that the dominant magnetic interactions take place within the dimers but such dimers also interact weakly with each other in a quite isotropic antiferromagnetic fashion. Analysing the crystal structure of **2**, we have found that the shortest distance between NO groups of different molecules is slightly shorter [d(N2···O5^{v})=4.89 Å; d(O2···O5^{v})=5.03 Å; v=$-x$, $1-y$, $-z$] than in radical **1**, occurring in a dimer geometry instead of in chains. This structural pattern therefore explains the observed magnetic characteristics of this molecular solid. The distances between NO groups of different dimers are larger than 5.24 Å and can be associated with the weaker interdimer antiferromagnetic interactions.

The experimental data for radical **3** can be fitted either by a 1D AFM model with $J/k_B=-0.62$ K or by the Curie–Weiss law with $\theta=-0.89$ K. Thus, such data clearly show the antiferromagnetic nature of the intermolecular interactions even though they do not have any singularity that permits us to distinguish the magnetic dimensionality of this molecular system.

In contrast, in the case of radical **4**, the presence of a broad maximum at 9 K in the χ *vs.* T plot strongly suggests a low magnetic dimensionality for this molecular solid. Actually, the data can be fitted to a dimer chain model[23] of $S=1/2$ molecular units with an intradimer exchange interaction of $J_1/k_B=-14.9$ K and an interdimer exchange interaction of $J_2/k_B=-10.5$ K. For radical **4**, the shortest distance between NO groups of different molecules [d(N10···O11^{ii})=3.69 Å, d(O11···O11^{ii})=3.81 Å, ii=$1-x$, $-y$, $-z$] occurs within the (1 0 0) layers among molecules belonging to neighbouring chains. The shortest distance between the spin-carrying units of different dimers [d(O15···O15^{vi})=4.61 Å; vi=$1-x$, $1-y$, $-z$] takes place along the b axis within the (1 0 0) plane. Moreover, the remaining distances between dimers are much longer, the lowest one being 5.65 Å. Therefore, all these facts explain the goodness of the experimental data to a dimer chain model for radical **4**. This magnetostructural correlation has short intra- and inter-dimer distances between NO units that are responsible for the strong antiferromagnetic couplings within and between the magnetic dimers. Both distances are clearly shorter than those observed for radicals **1** and **2** in agreement with the stronger antiferromagnetic couplings observed for **4**.

The χ *vs.* T plot of radical **5** shows a broader maximum at *ca.* 50 K indicating again a low dimensionality with a very strong antiferromagnetic interaction. The experimental data can be fitted to a simple dimer model with strong AFM ($J/k_B=-42.3$ K) interactions.[24] An additional Curie tail ($C=0.0043$ emu K mol^{-1}) is necessary to fit the low temperature values, which takes into account possible crystal surface effects or the presence of dislocations in the crystals. The strength of the intradimer interaction is remarkable, since it is one of the largest reported to date for a purely organic compound.

As mentioned previously in the description of the molecular packing of radical **5**, there are molecules linked by C—H···O—N hydrogen bonds that clearly form dimeric entities. The shortest distance between the spin-carrying units for radical **5** occurs inside these dimers [d(O11···O11^{iii})=3.37 Å; iii=$1-x$, $1-y$, $1-z$]. This short intermolecular distance is the shortest one observed in this family of radicals and explains the strong intermolecular magnetic interaction observed for radical **5**.

From the magnetostructural study it has been possible to establish a complete correlation between the solid state magnetic properties and the molecular arrangement in the crystals for all the radicals studied. Table 3 summarizes the main features of the structure and magnetic behaviour for radicals **1**, **2**, **4** and **5** showing in addition that the structural dimensionalities, based on packing motifs linked by hydrogen bonds, are different from the magnetic dimensionalities.

It also seems clear that the magnitude of exchange interactions between radical molecules in these molecular solids strongly decreases as the mean intermolecular distances

Table 3 Summary of structural and magnetic dimensionalities of radicals **1**, **2**, **3** and **5** together with the most relevant intermolecular contacts from the structural and magnetic points of view. See text for symmetry operations

compound	structural dimensionality[a]	structurally relevant contacts	magnetic dimensionality[b]	magnetically relevant contacts
1	2D	d(H11D···O14^{i})=2.64 Å	1D, regular chains	
		d(H7···O14^{ii})=2.66 Å	($J/k_B=-0.95$ K)	d(O14···O10^{iv})=5.39 Å[c]
2	2D	d(H14···O2^{i})=2.47 Å	0D AFM, dimers	
		d(H44···O5^{ii})=2.55 Å	($J/k_B=-1.82$ K)	d(O2···O5^{v})=5.03 Å[d]
4	2D	d(H8···O15^{i})=1.72 Å	1D, dimer chains	
		d(H134···)15^{ii})=2.71 Å	($J/k_B=-14.9$ K)	d(O15···O15^{vi})=4.61 Å
			($J_2/k_B=-10.5$ K)	d(O11···O11^{ii})=3.81 Å[e]
5	1D	d(H7···O11^{i})=2.22 Å	0D, dimers	
			($J/k_B=-42.3$ K)	d(O11···O11^{iii})=3.37 Å

[a]Based on the observed packing motifs linked by H···O hydrogen bonds with distances shorter than 2.8 Å. [b]Based on the fits of experimental magnetic data to magnetic models. Figures in parentheses are the strengths of dominant magnetic exchange interactions which are in all cases antiferromagnetic. [c]The corresponding O···N contact is shorter at d(O14···N9^{iv})=4.94 Å. [d]The corresponding O···N contact is shorter at d(N2···O5^{v})=4.89 Å. [e]The corresponding O···N contact is shorter at d(N10···O119^{ii})=3.69 Å.

between ONCNO units increases, being insignificant for O···O distances larger than 6.0 Å. Moreover, the AFM nature of such interactions can be rationalized by the McConnell I mechanism, through the contacts of atoms with the same sign of spin density, that belong to the NO units carrying the large spin density. An alternative but coincident rationalization of such magnetic interactions can be provided by the overlap of the SOMOs of neighbouring molecules.[13]

This research was financially supported by the C.I.C. y T. (Grant, MAT 94-0797), Spain and the Generalitat de Catalunya (Grant, SGR 95/00507). O. J. and J. C. thank also the Generalitat de Catalunya for the award of doctoral fellowships.

References

1 M. Tamaura, Y. Nakazawa, D. Shiomi, K. Nozawa, Y. Hosokoshi, M. Ishikawa, M. Takahashi and M. Kinoshita, *Chem. Phys. Lett*., 1991, **186**, 401.
2 (*a*) J. Veciana, J. Cirujeda, C. Rovira and J. Vidal-Gancedo, *Adv. Mater*., 1995, **7**, 221; (*b*) J. Cirujeda, C. Rovira and J. Veciana, *Synth. Met*., 1995, **71**, 1799; (*c*) J. Cirujeda, E. Hernández-Gasió, F. Lanfranc de Panthou, J. Laugier, M. Mas, E. Molins, C. Rovira, J. J. Novoa, P. Rey and J. Veciana, *Mol. Cryst. Liq. Cryst*., 1995, **271**, 1.
3 (*a*) H. Hernández-Gasió, M. Mas, E. Molins, C. Rovira and J. Veciana, *Angew. Chem., Int. Ed. Engl*., 1993, **32**, 882; (*b*) J. Cirujeda, E. Hernández-Gasió, C. Rovira, J. L. Stanger, P. Turek and J. Veciana, *J. Mater. Chem*., 1995, **5**, 243.
4 J. Cirujeda, M. Mas, E. Molins, F. Lanfranc de Panthou, J. Laugier, J. G. Park, C. Paulsen, P. Rey, C. Rovira and J. Veciana, *J. Chem. Soc., Chem. Commun*., 1995, 709.
5 T. Sugawara, M. M. Matsuskita, A. Izuoka, N. Wada, N. Takeda and M. Ishikawa, *J. Chem. Soc., Chem. Commun*., 1994, 1723.
6 R. Taylor and O. Kennard, *J. Am. Chem. Soc*., 1982, **104**, 5063.
7 (*a*) J. A. R. P. Sarma and G. R. Desiraju, *Acc. Chem. Res*., 1986, **19**, 222; (*b*) G. R. Desiraju, in *Organic Solid State Chemistry*, ed., G. R. Desiraju, Elsevier, 1987, p. 519; (*c*) J. A. R. P. Sarma and G. R. Desiraju, *Chem. Phys. Lett*., 1985, **117**, 160.
8 G. R. Desiraju, in *Organic Solid State Chemistry*, ed., G. R. Desiraju, Elsevier, 1987, p. 539.
9 N. W. Thomas and G. R. Desiraju, *Chem. Phys. Lett*., 1984, **110**, 99.
10 J. H. Osiecki and E. F. Ullman, *J. Am. Chem. Soc*., 1968, **90**, 1078; E. F. Ullman, J. H. Osiecki, D. G. B. Boocock and R. J. Darcy, *J. Am. Chem. Soc*., 1972, **94**, 7049.
11 M. Lamchen and T. W. Mittag, *J. Chem. Soc. C*, 1966, 2300.
12 (*a*) H. M. McConnell, *J. Phys. Chem*., 1963, **39**, 1910; (*b*) J. B. Goodenough, *Magnetism and the Chemical Bond*, Interscience, New York, 1963, p. 163; (*c*) H. M. McConnell, *Proc. R. A. Welch Found*, Conf. Chem. Res., 1967, **11**, 144.
13 In some aspects the McConnell I mechanism is a restatement of concepts introduced many years before by Heitler and London. Thus, dominant contact of atoms of two neighbouring molecules with spin densities having the same sign is equivalent to a non-zero overlap integral between their singly occupied molecular orbitals (SOMO) because such SOMOs are located on those atoms.
14 M. S. Davis, K. Morokuma and R. W. Kreilick, *J. Am. Chem. Soc*., 1974, **96**, 652.
15 J. A. D'Anna and J. H. Wharton, *J. Chem. Phys*., 1970, **53**, 4047.
16 (*a*) M. S. Davis, K. Morokuma and R. W. Kreilick, *J. Am. Chem. Soc*., 1972, **94**, 5588; (*b*) J. W. Neely, G. F. Hatch and R. W. Kreilick, *J. Am. Chem. Soc*., 1974, **96**, 652.
17 (*a*) J. Veciana, J. Cirujeda and O. Jürgens, Manuscript in preparation; (*b*) J. Cirujeda, Ph D Thesis, 1997, Universitat Ramon Llull.
18 C. W. Wang and S. F. Watkins, *J. Chem. Soc., Chem. Commun*., 1973, 888.
19 (*a*) J.-L. Stagner, Doctoral Thesis, 1995, Université Louis Pasteur de Strasbourg; (*b*) Y. Hosokoshi, Doctoral Thesis, 1995, University of Tokyo.
20 N. Ramasubbu, R. Parthasarathy and P. Murray-Rust, *J. Am. Chem. Soc*., 1986, **108**, 4308.
21 G. R. Desiraju, *Acc. Chem. Res*., 1991, **24**, 290.
22 The equation used to fit the data corresponds to a modified Bleaney–Bowers equation which includes a multiplying term to take account of intradimer interactions: $\chi = [Ng^2\mu_B{}^2/3k(T-\theta)][1+(1/3)\exp(-2J/kT)]^{-1}$. See R. L. Carlin in *Magnetochemistry*, Springer Verlag, Berlin, 1986, p. 88.
23 T. Barnes and J. Riera, *Phys. Rev. B*, 1994, **50**, 6817.
24 However, the fitting of the experimental data for **5** is slightly improved if the same model as for radical **2** is employed, with an intradimer interaction of $J/k_B = -50.1$ K and an additional interdimer term of $\theta = +10.4$ K, corresponding to the magnetic interactions among the dimers.

Paper 7/00589J; *Received* 27*th January*, 1997